

## Measurement of the Current-Density Profile and Plasma Dynamics in the Reversed-Field Pinch

D. L. Brower, W. X. Ding, and S. D. Terry

*Electrical Engineering Department, University of California at Los Angeles, Los Angeles, California 90095*

J. K. Anderson, T. M. Biewer, B. E. Chapman, D. Craig, C. B. Forest, S. C. Prager, and J. S. Sarff

*Physics Department, University of Wisconsin—Madison, Madison, Wisconsin 53706*

(Received 29 January 2002; published 23 April 2002)

First measurements of the current-density profile in the core of a high-temperature reversed-field pinch are presented. The current-density profile is observed to peak during the sawtooth cycle and broaden promptly at the crash. This change in profile can be linked to magnetic relaxation and the dynamo which is predicted to drive antiparallel current in the plasma core. For high-confinement discharges, the dynamo is suppressed and the current-density profile is observed to strongly peak.

DOI: 10.1103/PhysRevLett.88.185005

PACS numbers: 52.55.Hc, 52.25.Fi, 52.25.Gj, 52.70.Gw

In several configurations of magnetically confined plasmas, the spatial structure of the current density is a major determinant of plasma behavior. In the reversed-field pinch (RFP), and related configurations in which the confining magnetic field is relatively small, the current-density gradient is predicted to drive fluctuations in the magnetic field. The fluctuations in turn drive transport of particles and energy across the confining magnetic field. Moreover, the fluctuations in part determine the current-density spatial profile through their production of current (the dynamo effect).

Thus, measurement of the time evolution of the radial profile of the mean current density (obtained after averaging over the poloidal and toroidal directions) is essential for an understanding of the fluctuations, transport, and dynamo physics. The effect of fluctuations on the current-density profile is particularly strong during the crash phase of the sawtooth oscillation in the RFP. During this sudden event, the fluctuations vary significantly and are believed to alter the current-density profile [1]. Conversely, the effect of the current density on fluctuations is particularly evident during improved confinement RFP plasmas [2,3]. In these plasmas, transport is reduced through modification of the electric field (and current-density) profile. The current density is altered, in a way to reduce fluctuations, by programming the electric field parallel to the edge magnetic field (known as pulsed parallel current drive, or PPCD).

In this Letter, we report the first measurement of the current-density profile during these two plasma conditions: sawtooth oscillation in standard RFP plasmas and improved confinement PPCD plasmas. To this end, we have developed a high-speed Faraday rotation polarimetry system to measure the internal magnetic field (and its rapid changes), from which the current density is evaluated.

We report two new results. Each result reflects the phenomenon that magnetic fluctuations in the RFP tend to flatten the current-density profile—the dynamo effect. First, we measure that the current density flattens during the crash phase of the sawtooth cycle, and peaks during the slow ramp phase of the cycle. This is consistent with

the expectation that the sawtooth crash is a sudden enhancement of the dynamo, leading to flattening of the current profile—the standard picture of magnetic relaxation. Second, we find that the parallel current density increases in the outer region of the plasma during PPCD, as expected, due to the edge parallel electric field which is applied to deliberately flatten the current profile. However, the current density also increases in the core, relative to standard plasmas. This apparently surprising increase can be explained by a reduction of the dynamo (anti)current drive in the core that should accompany reduced magnetic fluctuations.

The diagnostic approach employed utilizes two distinct but collinear far-infrared (FIR) laser beams to probe the plasma [4]. The probing beams are frequency offset and their polarizations are set to counterrotating circular. Because of plasma birefringence, each beam experiences a different value of refractive index upon propagation through the plasma. The difference in refractive index is related to the Faraday rotation angle,  $\Psi$ , by the relation

$$\begin{aligned}\Psi &= \frac{\lambda_0^2 e^3}{8\pi^2 c^3 \epsilon_0 m_e^2} \int n_e B_{\parallel} dz \\ &= 2.62 \times 10^{-13} \lambda_0^2 \int n_e B_{\parallel} dz,\end{aligned}\quad (1)$$

where  $B_{\parallel}$  is the component of the magnetic field parallel to the vertically propagating FIR beams,  $n_e$  is the electron density, and  $\lambda_0$  is the laser wavelength, all in MKS units. Since  $n_e$  is known from interferometry, the poloidal magnetic field can be determined from the solution of the above equation ( $B_{\parallel} = B_{\theta} \cos\theta$ , where  $\theta$  is the angle between the polarimeter chord and  $B_{\theta}$ ). The toroidal current density is then obtained by using Ampere's law,  $\nabla \times \mathbf{B} = \mu_0 \mathbf{J}$ . The above equation for  $\Psi$  corresponds to half the phase difference between right-hand and left-hand circularly polarized waves in a plasma.

This experimental approach, originally proposed in 1978 by Dodel and Kunz [5], produces a phase measurement with time response limited by the frequency offset of the

two probing beams. The FIR laser beams are at nominal wavelength  $432 \mu\text{m}$  (694 GHz) and operated at a difference frequency of  $\Delta\omega/2\pi \approx 750 \text{ kHz}$ . The 11 chord data are routinely sampled at 1 MHz with the difference frequency being aliased down to 250 kHz. This results in a maximum time response of  $4 \mu\text{s}$ , which is sufficient to follow the dynamics of interest in MST. Initial work on a single-channel system using a similar technique was done on ZT-40M [6]. A digital phase comparator technique is employed to extract the phase information for both the polarimeter and interferometer [7]. Typical polarimeter system rms noise levels are  $\approx 0.1^\circ$  at 100 kHz bandwidth. To obtain the necessary polarimetry and interferometry data, the system is first operated in polarimeter mode for 20–30 similar shots and then converted to interferometer mode for a similar number of shots to obtain the electron density. The data are ensemble averaged over the sawtooth cycle producing the average profile change over approximately 400 sawtooth events.

The MST reversed-field pinch is Ohmically heated and has major radius  $R_0 = 1.50 \text{ m}$  and limiter radius  $a = 0.51 \text{ m}$ . Data presented are for plasmas with plasma current  $I_p = 400 \text{ kA}$  and nominal electron density  $n_e = 1 \times 10^{19} \text{ m}^{-3}$  using a deuterium working gas.

Faraday rotation data analysis presented in this paper involves the use of three independent techniques, of increasing complexity, to arrive at information on the current-density distribution. The simplest analysis yields the central current density (from the slope of the Faraday rotation profile at the center), the next analysis employs a fitting method to solve Eq. (1) and yields the toroidal current-density profile, and the most complex analysis utilizes a two-dimensional equilibrium reconstruction code (solving the Grad-Shafranov equation) to yield the current density as a function of magnetic surface coordinate. All three techniques provide consistent information on  $J(r)$ .

First, for chords with impact parameter ( $x$ ) close to the magnetic axis,  $B_{\parallel} (= B_{\theta} \cos\theta)$  becomes localized to the plasma core since contributions to  $\cos\theta$  along the chord come only from the plasma center. Through the use of Ampere's law in the limit  $r \Rightarrow 0, x \Rightarrow 0$ , Eq. (1) can be rewritten in terms of the current density on axis,  $J(0)$ , as

$$J(0) = \frac{2}{\mu_0 c_F} \frac{d\Psi}{dx} \frac{1}{\int n_e f(r, \alpha) dz}, \quad (2)$$

where  $c_F$  is a constant, and  $f(r, \alpha)$  represents the current profile shape [estimated from the total current  $I_p = J(0) \int 2\pi r f(r, \alpha) dr$ ]. This leaves us with a relation for  $J(0)$  which is proportional to the slope of the Faraday rotation signal across the magnetic axis,  $d\Psi/dx$ .

Since the density is known from independent interferometry measurements, Eq. (1) can be solved directly for the poloidal magnetic field. This involves spline fitting and inversion of both the interferometry and polarimetry data. Although the spline-fitting inversion technique is most general, a parametrized functional fitting method is the second

approach used herein to handle the polarimetry data due to the limited number of chords and sensitivity to errors. The zero order (cylindrical) current-density profile shape chosen is of the form  $J_{\phi} = J(0)[1 - (r/a)^2]^{\alpha}$ , with free parameters  $J(0)$  and  $\alpha$ . The functional estimate for the toroidal current density is used to calculate  $B_{\theta}$  in a cylindrical geometry from Ampere's law according to

$$\mu_0 J_{\phi} = \frac{1}{r} \frac{d[rB_{\theta, \text{cyl}}(r)]}{dr}. \quad (3)$$

Then the large aspect ratio expansion is used to include toroidal curvature effects, leading to a correction term for the poloidal magnetic field:

$$B_{\theta}(r) = B_{\theta, \text{cyl}}(r) \left[ 1 - \left( \frac{r}{R_0} + \frac{d\delta(r)}{dr} \right) \cos\theta \right], \quad (4)$$

where  $\delta(r)$  is the Shafranov shift, which is a radially varying shift of the flux surfaces due to toroidal curvature of the plasma [8]. The Shafranov shift at the magnetic axis,  $\delta(0)$ , is a free parameter largely determined by the zero crossing point of the Faraday rotation profile and a quadratic dependence with minor radius is assumed,  $\delta(r) = \delta(0)[1 - (r/a)^2]$ . A nonlinear least-squares fitting routine is used to adjust the free parameters and optimize the fit to the measured Faraday rotation profile along with the constraint of matching the total integrated current,  $I_p$ , as determined by Rogowski loops.

The third technique involves modeling using the equilibrium reconstruction code MSTFIT [9] which provides a toroidal equilibrium solution which best fits all of the magnetic and pressure data available. We also compare with a cylindrical equilibrium model reconstruction constrained by external magnetic measurements only [10,11]. This simple model has been widely used in RFP research.

Typical MST fast-polarimetry data for a standard sawtooth discharge are shown in Fig. 1. All chords show

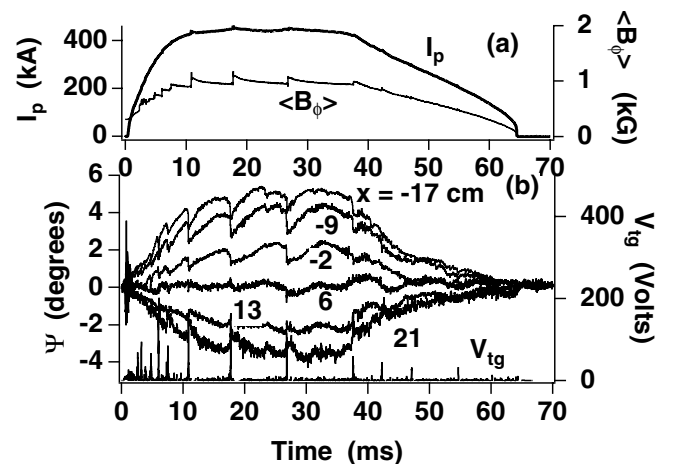


FIG. 1. (a) Plasma current and average toroidal magnetic field. (b) Faraday rotation signals for standard Ohmic MST plasma. Sawtooth crashes are marked by spikes in the toroidal gap voltage,  $V_{tg}$ . Vacuum vessel center corresponds to  $x = 0$ .

a strong correlation with the sawtooth cycle, even during the setup phase of the discharge (0–10 ms). Sawtooth crashes, characterized by changes in toroidal flux, are denoted by prompt increases in the average toroidal field,  $\langle B_\phi \rangle$ . As expected, the Faraday rotation angle changes sign about the magnetic axis due to a change in the direction of the poloidal magnetic field with respect to the polarimeter chords. The typical sawtooth crash or relaxation time scale is measured to be  $\approx 100 \mu\text{s}$ . The RFP sawtooth crash represents a discrete dynamo event. Since the polarimeter measures the line-integrated product of density and magnetic field [see Eq. (1)], changes observed in the Faraday rotation signal likely correspond to changes in both parameters. With these results, it is now possible to extract information on the plasma poloidal magnetic field, current density profile, and their temporal evolution.

Here, for the first time, direct experimental measurement shows that the current density on axis drops by 20% during the relaxation towards the Taylor minimum energy state [12]. Comparison of  $J(0)$  estimated from Eq. (2) with  $J(0)$  from the simple cylindrical equilibrium model [10,11] is shown in Fig. 2, and the two agree quite well in both absolute value and temporal history. The agreement, within measurement errors of  $\sim 10\%$ , bolsters confidence in both the measurement technique and the cylindrical equilibrium model. The current-density decrease at the sawtooth crash can potentially be explained by the MHD dynamo which is predicted to drive antiparallel current in the plasma core [1].

Faraday rotation profiles, taken from the ensembled data, at times immediately before ( $-0.25$  ms) and after ( $+0.25$  ms) the sawtooth crash are shown in Figs. 3(a) and 3(b). The magnetic axis corresponds to the point where  $\Psi = 0$  and is shifted approximately 4–5 cm outward from the center of the conducting boundary. Reduced slope ( $d\Psi/dx$ ), proportional to reduced current density on axis, is evident for the central chords after the sawtooth crash. The maximum rotation angle (absolute value) is larger on the inboard side due to the toroidal geometry.

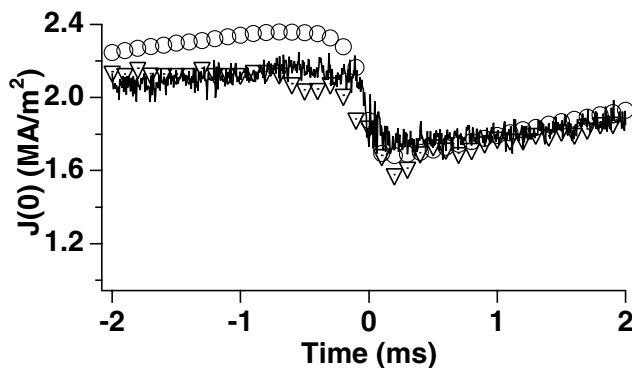


FIG. 2. Comparison of  $J(0)$  through the sawtooth cycle as determined from Eq. (2) (solid line), cylindrical equilibrium model (open circles,  $\beta = 7\%$ ), and functional fit analysis (open triangles). Ensembled data are used.

By use of the functional fitting technique, toroidal current density ( $J_\phi$ ) profiles corresponding to times before and after the sawtooth crash are generated and shown in Fig. 4(a). Corresponding fits to the measured Faraday profiles are shown as solid lines in Figs. 3(a) and 3(b). The toroidal current density indicates a clear reduction in the plasma core,  $r < 0.2$  m, and increase towards the outside,  $r > 0.2$  m, immediately after the sawtooth crash. The decreased interior current density is in excellent agreement with Fig. 2. After the crash, the flattened profile begins to slowly narrow and peak on axis until the next sawtooth or relaxation event. The toroidal current density is very small in the edge where the toroidal field reverses and the parallel direction is predominantly poloidal.

The toroidal current density determined from the equilibrium reconstruction code MSTFIT is shown in Fig. 4(b). Inputs to the toroidal equilibrium code include the external magnetics, pressure profiles, motional Stark effect measurements of  $B(0)$ , as well as the Faraday rotation data. The corresponding fits to the Faraday rotation profile [see Figs. 3(a) and 3(b)] are nearly indistinguishable from the functional fit result, and both match the measured Faraday rotation profile quite well. The current-density profile is very sensitive to changes in the Faraday profile. Differences in toroidal current-density shape between the functional fit and equilibrium reconstruction approaches provide an indication of errors in the resulting profiles. Both results show the same general features of a peaking current-density distribution which flattens significantly at the sawtooth crash.

High-confinement plasmas are achieved in MST by inductively driving poloidal (parallel) current in the edge through PPCD. PPCD acts to suppress sawteeth and the  $m = 0, 1$  resistive tearing modes that limit energy and particle confinement in RFP plasmas [2,3]. Field reversal is maintained via external drive rather than the dynamo. For these improved-confinement plasmas, both the energy and the particle confinement time are observed to increase tenfold [2,3]. As shown in Fig. 4, from both the functional fit and MSTFIT equilibrium reconstruction, distinct peaking of the toroidal current density in the plasma core is observed

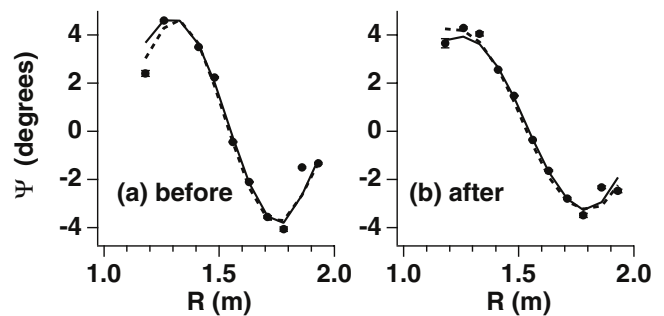


FIG. 3. Measured Faraday rotation profiles at times (a) 0.25 ms before and (b) 0.25 ms after the sawtooth crash. Symbols represent the measurement points (error bars approximately equal symbol size), solid lines the functional fit, and dashed lines the MSTFIT matching.

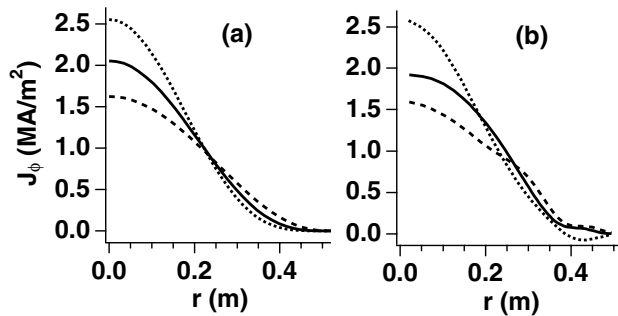


FIG. 4. Toroidal current-density profile generated by (a) functional fit approach and (b) MSTFIT for times 0.25 ms before the sawtooth crash (solid line), 0.25 ms after the sawtooth crash (long dashed line), and during PPCD (short dashed line).

during PPCD. The current density on axis increases by 30% compared to the presawtooth crash  $J_\phi(0)$  value while the current tends to decrease at the edge. This peaking may be explained by a reduction in the dynamo effect and the emergence of high-energy runaway electrons [13] that accompany the fluctuation reduction (as well as by increased conductivity due to increasing electron temperature) [2].

The parallel current density  $J_\parallel(r)$  and  $\lambda(= \mu_0 a J_\parallel / B)$  profiles output from the toroidal equilibrium reconstructions are shown in Fig. 5, where  $\lambda$  is the normalized measure of the parallel current density that determines tearing mode stability and is a spatial constant for the minimum energy Taylor state. We observe that both the  $J_\parallel$  and  $\lambda$  profiles experience a slow peaking during the sawtooth rise phase, and a sudden flattening during the crash. This is again consistent with the MHD model of the dynamo, which drives the plasma toward a more stable (flatter  $\lambda$ ) state during the crash. As the  $\lambda$  profile peaks, magnetic fluctuations increase, eventually becoming large enough to drive the profile relaxation. During PPCD, the parallel current density appears to increase across the entire profile being more peaked on axis than the presawtooth crash case. However, for  $r > 0.3$  m,  $J_\parallel(r)$  is quite similar to the postsawtooth crash case. This is also reflected in  $\lambda(r)$ , indicating the profile is being maintained closer to the more stable postcrash relaxed state by the application of PPCD.

In summary, the core current-density profile has been measured for the first time in a high-temperature reversed-field pinch plasma. The current density, as determined from both measurement and equilibrium reconstruction, is peaked on axis with  $J(0)$  increasing throughout the sawtooth cycle ramp phase. At the crash, the profile promptly flattens consistent with relaxation towards the Taylor minimum energy state and dynamo theory which predicts counter-current drive in the core and cocurrent drive in the edge. For high-confinement MST plasmas, where edge parallel current is inductively driven, the current-density profile becomes more peaked. This somewhat surprising result can be explained by the reduction of the fluctuation-induced

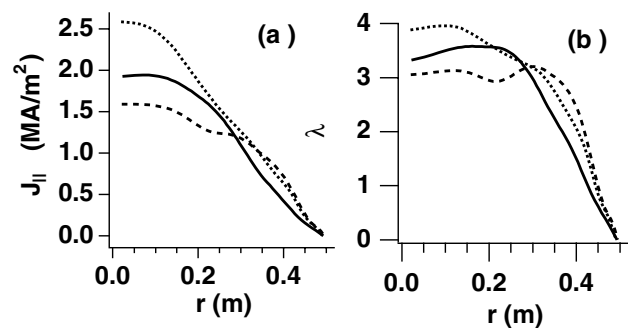


FIG. 5. (a) Parallel current-density and (b)  $\lambda$  profiles for times 0.25 ms before the sawtooth crash (solid line), 0.25 ms after the sawtooth crash (long dashed line), and during PPCD (short dashed line), generated from MSTFIT equilibrium reconstruction code.

dynamo effect (that tends to flatten the profile). Future work will focus on using the polarimeter to directly measure the core magnetic fluctuations and to relate changes in fluctuation amplitude to gradients in the current-density distribution. In addition, core measurements of the fluctuating flow velocity along with magnetic fluctuation measurements will be used to directly determine the core MHD dynamo and assess consistency with Ohm's law and the measured current-density profile. Improved understanding of MHD stability in the RFP configuration should lead to further increases in confinement and overall machine performance.

The authors are grateful for the contributions of Dr. D. J. Holly, Dr. N. E. Lanier, and the MST group. This work is supported by the U.S. Department of Energy.

- 
- [1] D. J. Den Hartog *et al.*, *Phys. Plasmas* **6**, 1813 (1999).
  - [2] B. E. Chapman *et al.*, *Phys. Rev. Lett.* **87**, 205001 (2001).
  - [3] N. E. Lanier *et al.*, *Phys. Rev. Lett.* **85**, 2120 (2000).
  - [4] D. L. Brower, W. X. Ding, and S. D. Terry, "Interior Magnetic Field Fluctuation and Profile Measurements on MST" (Plenum Press, New York, to be published).
  - [5] G. Dodel and W. Kunz, *Infrared Phys.* **18**, 773 (1978).
  - [6] R. M. Erickson, Los Alamos National Laboratory Report LA-10731-T, 1986.
  - [7] Y. Jiang, D. L. Brower, and L. Zeng, *Rev. Sci. Instrum.* **68**, 902 (1997).
  - [8] J. P. Friedberg, *Ideal Magnetohydrodynamics* (Plenum Press, New York, 1987).
  - [9] J. K. Anderson, Ph.D. dissertation, University of Wisconsin-Madison, Madison, 2001.
  - [10] J. S. Sarff, N. E. Lanier, S. C. Prager, and M. R. Stoneking, *Phys. Rev. Lett.* **78**, 62 (1997).
  - [11] V. Antoni, P. Martin, and S. Ortolani, *Nucl. Fusion* **29**, 1759 (1989).
  - [12] J. B. Taylor, *Phys. Rev. Lett.* **33**, 1139 (1974).
  - [13] R. O'Connell *et al.*, *Bull. Am. Phys. Soc.* **46**, 109 (2001).